Proceedings of the XI DINAME, 28th February - 4th March, 2005 – Ouro Preto – MG – Brazil
Edited by D.A. Rade and V. Steffen Jr.

REDUCTION OF VISCOELASTIC FINITE ELEMENT MODELS BASED ON INTERNAL VARIABLES

Marcelo A. Trindade
Department of Mechanical Engineering, São Carlos School of Engineering, University of São Paulo, .
Av. Trabalhador São-Carlense, 400, São Carlos-SP, 13566-590, Brazil .
trindade@sc.usp.br

Abstract: *Hybrid active-passive damping treatments combine the reliability, low cost and robustness of viscoelastic damping treatments and the high performance, modal selective and adaptive piezoelectric active control. The main difficulty when associating such active and passive damping mechanisms is that active controllers are generally very sensitive to system changes while viscoelastic materials properties are highly frequency-dependent. In addition, most modern control techniques require a time-domain model representation. This can be solved through the use of internal variables viscoelastic models, such as the Anelastic Displacements Fields (ADF) and the Golla-Hughes-McTavish (GHM). Unfortunately, they increase considerably the order of the model as they add internal variables to the system to compensate for frequency dependence. Hence, a model reduction method is normally required. The present work presents alternative reduction methods for internal variables-based viscoelastic FE models. This is done through a physical interpretation of the dissipative modes and their coupling with structural vibration modes in the second-order models. The resulting reduced-order models are then compared in terms of performance and computational efficiency for passive constrained layer damping treatments.*
Keywords: *vibration control, piezoelectric materials, viscoelastic materials, internal variables, model reduction.*

1 Introduction

Several studies have shown that combining active and passive control is often a better solution for structural vibration damping. The main reason stems from the possibility of combining the reliable, low cost and robust passive damping and the high performance, modal selective and adaptive active control. One of the most promising active-passive damping mechanisms is obtained by including piezoelectric actuators in the standard viscoelastic constrained layer damping treatments. These active-passive treatments may be optimized by varying the relative positions of viscoelastic layers and piezoelectric actuators (Trindade and Benjeddou, 2002). The main difficulty when associating such active and passive damping mechanisms is that active controllers are generally very sensitive to system changes while viscoelastic materials properties are highly frequency-dependent. In addition, most modern control techniques require a time-domain model representation. Therefore, methods such as the Anelastic Displacements Fields (ADF) proposed by Lesieutre and Bianchini (1995) and Golla-Hughes-McTavish (GHM) proposed by Golla and Hughes (1985) and McTavish and Hughes (1993) have been applied to this active-passive treatments, since they are able to model the frequency dependence of stiffness and damping properties of viscoelastically damped structures in the time-domain (Trindade, Benjeddou and Ohayon, 2000). It was shown that both ADF and GHM are effective for time-domain analyses of highly damped structures. Unfortunately, they increase considerably the order of the model as they add internal variables to the system to compensate for frequency dependence. Hence, a model reduction method is normally required.

There are mainly three strategies published in the literature for the reduction of viscoelastic finite element (FE) models with internal variables. The first one consists in applying some reduction method to the undamped structural FE model before adding the internal variables, which has the advantage of handling smaller matrices but generally leads to erroneous or less precise estimations of viscoelastic damping. Friswell and Inman (1999) considered reducing the order of the physical FE model, through a system equivalent reduction expansion process (SEREP), before and after assembly, previous to introducing the extra dissipation coordinates for the GHM method. The second reduction strategy consists in applying a reduction method to the second order augmented FE model, after inclusion of internal variables. Park, Inman and Lam (1999) have studied Guyan reduction method to reduce the order of a FE model augmented by GHM viscoelastic dissipation coordinates, but they show that the method perform poorly. The third strategy is based on the application of a reduction method to the augmented state space system, that is after inclusion of the internal variables and transformation to the state space form. This has the advantage of allowing the application of modern reduction methods, developed for state space systems, such as internal balancing method. Park, Inman and Lam (1999) and Friswell and Inman (1999) applied an internal balancing method to a state space system augmented by GHM dissipation coordinates. Friswell and Inman (1999) also applied eigensystem truncation for comparison.

The present work presents an alternative reduction method for internal variables-based viscoelastic FE models. This is done through a physical interpretation of the dissipative modes and their coupling with structural vibration modes in the second-order model. The objective is to allow a reduction of the extra dissipative coordinates before transformation to the state space system, so as to provide faster computations on the reduction of the state space system as a second reduction phase. The resulting reduced-order model is then compared in terms of performance and computational efficiency with full-order models for passive constrained layer damping treatments.

2 Finite element model

In a previous work (Trindade, Benjeddou and Ohayon, 2001a), a finite element model able to deal with sandwich beams with viscoelastic core and multilayer faces was presented. The laminated faces were supposed to behave as Bernoulli-Euler beams while Timoshenko hypothesis was retained for the core, to allow shear strains to occur in the viscoelastic material layer. Three-dimensional constitutive matrices are considered for each material and then transformed according to the layer orientation in the *xy* plane. The transformed three-dimensional constitutive matrices are finally reduced using the *xy* plane-stress assumption. Consequently, composite material orientation is properly accounted for in the FE model. The assembled equations of motion may be written as (Trindade, Benjeddou and Ohayon, 2001a)

$$\mathbf{M}\ddot{\mathbf{q}} + \mathbf{D}\dot{\mathbf{q}} + [\mathbf{K}_e + \mathbf{K}_v]\mathbf{q} = \mathbf{F} \tag{1}$$

where $\mathbf{q}$ is the dofs vector, composed by the nodal axial mean and relative displacements, deflections and bending rotations. $\dot{\mathbf{q}}$ and $\ddot{\mathbf{q}}$ are respectively the velocity and acceleration vectors. $\mathbf{M}$ is the mass matrix, $\mathbf{D}$ is a viscous damping matrix introduced *a posteriori* and $\mathbf{F}$ is a mechanical perturbation input. $\mathbf{K}_v$ is the part of the stiffness matrix corresponding to the contribution of the viscoelastic material, which is frequency-dependent, and $\mathbf{K}_e$ is the stiffness matrix corresponding to the remaining contributions in the structure.

The frequency-dependence of the viscoelastic material is modeled through the Lesieutre's ADF model (Lesieutre and Bianchini, 1995). The ADF model is based on a separation of the viscoelastic material strains in an elastic part, instantaneously proportional to the stress, and an anelastic part, representing material relaxation. This could be applied to Eq. (1) by replacing the dof vector $\mathbf{q}$ by $\mathbf{q}^e = \mathbf{q} - \sum_i \mathbf{q}_i^d$ in the viscoelastic strain energy. $\mathbf{q}^e$ and $\mathbf{q}_i^d$ represent the dof vectors associated with the elastic and anelastic strains, respectively. Adding a system of equations describing the time-domain evolution of the dissipative dof $\mathbf{q}_i^d$ to Eq. (1), we get

$$\mathbf{M}\ddot{\mathbf{q}} + \mathbf{D}\dot{\mathbf{q}} + (\mathbf{K}_e + \mathbf{K}_v^\infty)\mathbf{q} - \mathbf{K}_v^\infty \sum_i \mathbf{q}_i^d = \mathbf{F} \tag{2}$$

$$\frac{C_i}{\Omega_i}\mathbf{K}_v^\infty \dot{\mathbf{q}}_i^d + C_i \mathbf{K}_v^\infty \mathbf{q}_i^d - \mathbf{K}_v^\infty \mathbf{q} = \mathbf{0} \tag{3}$$

where $\mathbf{K}_v^\infty = G_\infty \bar{\mathbf{K}}_v$, for $G_\infty = G_0(1 + \sum_i \Delta_i)$ and $C_i = (1 + \sum_i \Delta_i)/\Delta_i$ (Lesieutre and Bianchini, 1995). ADF parameters G_0, Δ_i and Ω_i are evaluated by curve-fitting of the measurements of $G^*(\omega)$, represented as a series of functions in the frequency-domain

$$G^*(\omega) = G_0 + G_0 \sum_i \Delta_i \frac{\omega^2 + \mathrm{j}\omega\,\Omega_i}{\omega^2 + \Omega_i^2} \tag{4}$$

The form of the series of functions used to construct $G^*(\omega)$ is well adapted to fit the behavior of complex modulus frequency-dependence for generic viscoelastic materials, which present strong frequency-dependence. Nevertheless, modern viscoelastic materials tend to be less frequency-dependent so as to maintain a high loss factor, and consequently being more effective in damping vibrations, over a wide frequency-range of interest. For such materials, a larger number of series must be used to provide a satisfactory curve-fit of complex modulus frequency-dependence. A more detailed analysis of curve-fitting will be presented later, but it is worthwhile advancing that for modern viscoelastic materials used for vibration damping more than 3 ADF series terms are generally required and the larger the number of ADF series terms considered the better fitting of materials properties is obtained. Notice however that there is one system of equations (3) for each ADF series term considered. Thus, there must be a compromise between the quality of material properties curve-fitting and the number of extra systems of equations included into the final augmented system. Since the extra dissipative dof $\mathbf{q}_i^d$ included for each ADF series term has the same dimension of $\mathbf{q}$, the dimension of the final augmented system will be 4 times that of the original FE system (considering 3 ADF series terms to represent frequency-dependence behavior).

It is worthwhile to notice also that in the case of a structure partially covered with the viscoelastic treatment, the viscoelastic stiffness matrix $\mathbf{K}_v$ will possess a number of rigid body modes, corresponding to the FE dof of the non-treated parts of the structure. Consequently, there will be a number of equations in Eq. (3) that will be automatically satisfied. Hence, the increase in the augmented system dimension will be also dependent on the percent of area covered with the viscoelastic material throughout the structure surface.

The rigid body modes of $\mathbf{K}_v$ can be eliminated through a modal decomposition $\mathbf{q}_i^d = \mathbf{T}_d \hat{\mathbf{q}}_i^d$ such that $\Lambda_d = \mathbf{T}_d^T \mathbf{K}_v^\infty \mathbf{T}_d$ and Eqs. (2) and (3) can be rewritten as

$$\mathbf{M}\ddot{\mathbf{q}} + \mathbf{D}\dot{\mathbf{q}} + (\mathbf{K}_e + \mathbf{K}_v^\infty)\mathbf{q} - \mathbf{T}_d \Lambda_d \sum_i \hat{\mathbf{q}}_i^d = \mathbf{F} \tag{5}$$

$$\frac{C_i}{\Omega_i}\Lambda_d \dot{\hat{\mathbf{q}}}_i^d + C_i \Lambda_d \hat{\mathbf{q}}_i^d - \Lambda_d \mathbf{T}_d^T \mathbf{q} = \mathbf{0} \tag{6}$$

The equations that are automatically satisfied correspond to the null eigenvalues in matrix Λ_d. Notice that these rigid body modes of $\mathbf{K}_v$ do not contribute to the overall structure damping. Hence, the null eigenvalues are eliminated from Λ_d and so are the corresponding eigenvectors from $\mathbf{T}_d$. Notice also that, in this case, a complete modal decomposition of $\mathbf{K}_v$

is required, hence for complex structures one should look for a selective decomposition alternative. Combination of Eqs. (5) and (6), leads to the following augmented system

$$\bar{\mathbf{M}}\ddot{\bar{\mathbf{q}}}+\bar{\mathbf{D}}\dot{\bar{\mathbf{q}}}+\bar{\mathbf{K}}\bar{\mathbf{q}}=\bar{\mathbf{F}} \tag{7}$$

with

$$\bar{\mathbf{M}}=\begin{bmatrix}\mathbf{M} & \mathbf{0}\\ \mathbf{0} & \mathbf{0}\end{bmatrix}\ ;\ \bar{\mathbf{D}}=\begin{bmatrix}\mathbf{D} & \mathbf{0}\\ \mathbf{0} & \mathbf{D}_{dd}\end{bmatrix}\ ;\ \bar{\mathbf{F}}=\begin{Bmatrix}\mathbf{F}\\ \mathbf{0}\end{Bmatrix}$$

$$\bar{\mathbf{K}}=\begin{bmatrix}\mathbf{K}_e+\mathbf{K}_v^{\infty} & \mathbf{K}_{ed}\\ \mathbf{K}_{ed}^T & \mathbf{K}_{dd}\end{bmatrix}\ ;\ \bar{\mathbf{q}}=\mathrm{col}\left(\mathbf{q},\ \hat{\mathbf{q}}_1^d,\ \ldots,\ \hat{\mathbf{q}}_n^d\right)$$

where,

$$\mathbf{D}_{dd}=\mathrm{diag}\left(\frac{C_1}{\Omega_1}\Lambda_d\ \cdots\ \frac{C_n}{\Omega_n}\Lambda_d\right)\ ;\ \mathbf{K}_{dd}=\mathrm{diag}\left(C_1\Lambda_d\ \cdots\ C_n\Lambda_d\right)\ ;\ \mathbf{K}_{ed}=\left[-\mathbf{T}_d\Lambda_d\ \cdots\ -\mathbf{T}_d\Lambda_d\right]$$

3 State space model construction

In order to eliminate the apparent singularity of the mass matrix of system (7) and to provide a transformation to an "elastic only" modal reduced model, Eq. (7) is rewritten in a state space form. Therefore, a state vector $\mathbf{x}$ is formed by the augmented vector $\bar{\mathbf{q}}$ and the time-derivative of the mechanical dofs vector $\dot{\mathbf{q}}$. The time-derivatives of the dissipative dofs $\mathbf{q}_i^d$ may not be considered since these variables are massless. This leads to

$$\begin{aligned}\dot{\mathbf{x}}&=\mathbf{A}\mathbf{x}+\mathbf{p}\\ \mathbf{y}&=\mathbf{C}\mathbf{x}\end{aligned} \tag{8}$$

where the perturbation vector $\mathbf{p}$ is the state distribution of the mechanical loads $\mathbf{F}$ and the output vector $\mathbf{y}$ is, generally, composed of the measured quantities, written in terms of the state vector $\mathbf{x}$ through the output matrix $\mathbf{C}$. The system dynamics is determined by the square matrix $\mathbf{A}$. These are

$$\mathbf{A}=\begin{bmatrix}\mathbf{0} & \mathbf{0} & \cdots & \mathbf{0} & \mathbf{I}\\ \frac{\Omega_1}{C_1}\mathbf{T}_d^T & -\Omega_1\mathbf{I} & & \mathbf{0} & \mathbf{0}\\ \vdots & & \ddots & & \mathbf{0}\\ \frac{\Omega_n}{C_n}\mathbf{T}_d^T & \mathbf{0} & & -\Omega_n\mathbf{I} & \mathbf{0}\\ -\mathbf{M}^{-1}(\mathbf{K}_e+\mathbf{K}_v^{\infty}) & \mathbf{M}^{-1}\mathbf{T}_d\Lambda_d & \cdots & \mathbf{M}^{-1}\mathbf{T}_d\Lambda_d & -\mathbf{M}^{-1}\mathbf{D}\end{bmatrix}$$

$$\mathbf{x}=\begin{bmatrix}\bar{\mathbf{q}}\\ \dot{\mathbf{q}}\end{bmatrix}\ ;\ \mathbf{p}=\begin{bmatrix}\mathbf{0}\\ \mathbf{M}^{-1}\mathbf{F}\end{bmatrix}\ ;\ \mathbf{C}=\begin{bmatrix}\mathbf{C}_{\bar{q}} & \mathbf{C}_{\dot{q}}\end{bmatrix}$$

where $\mathbf{C}_{\bar{q}}$ and $\mathbf{C}_{\dot{q}}$ are output matrices relative to augmented dofs vector $\bar{\mathbf{q}}$ and mechanical dofs derivatives $\dot{\mathbf{q}}$, respectively.

4 Model reduction

It is evident from Eq. (7) that inclusion of dissipative dof greatly increases the dimension of the FE model, even for a partial treatment, corresponding to a great increase also in the final state space model (Eq. (8)). Since our final objective is to apply the state space model for control design and optimization, leading to CPU-demanding computations for a large number of candidate configurations, some model reduction is required. Hence, in this section some techniques are presented to provide a reduced-order state space model, which dimension is small enough to allow application to control design and optimization and that is still able to well represent the viscoelastic damping of the structure.

4.1 State space model reduction

In principle, all reduction techniques for state space systems may be applied to Eq. (8). The most standard ones are the reduction to modal coordinates and the reduction via internal balancing methods. While the latter leads to more precise results for a given input and output configuration, the former is independent of input and output configurations and also allow faster computations. Details on modal reduction can be found in (Trindade, Benjeddou and Ohayon, 2001b) and are briefly repeated here. Details on reduction via internal balancing methods can be found in (Park, Inman and Lam, 1999).

4.1.1 Complex modal reduction

In what follows a complex-based modal reduction is applied to the state space system (8), neglecting the contributions of the viscoelastic relaxation modes and the elastic modes related to eigenfrequencies out of the frequency-range considered. Hence, the eigenvalues matrix Λ and, left $\mathbf{T}_l$ and right $\mathbf{T}_r$, eigenvectors of Eq. (8) are first evaluated from

$$\mathbf{A}\mathbf{T}_r=\Lambda\mathbf{T}_r\ ;\ \mathbf{A}^T\mathbf{T}_l=\Lambda\mathbf{T}_l \tag{9}$$

so that $\mathbf{T}_l^T\mathbf{T}_r = \mathbf{I}$, then decomposed as following

$$\Lambda = \begin{bmatrix} \Lambda_r & \mathbf{0} & \mathbf{0} \\ \mathbf{0} & \Lambda_{ne} & \mathbf{0} \\ \mathbf{0} & \mathbf{0} & \Lambda_{nd} \end{bmatrix} \; ; \; \mathbf{T}_l = [\mathbf{T}_{lr} \; \mathbf{T}_{lne} \; \mathbf{T}_{lnd}] \; ; \; \mathbf{T}_r = [\mathbf{T}_{rr} \; \mathbf{T}_{rne} \; \mathbf{T}_{rnd}] \tag{10}$$

where Λ_r is the retained elastic eigenvalues matrix and $\mathbf{T}_{lr}$ and $\mathbf{T}_{rr}$ are its left and right corresponding eigenvectors matrices, respectively. Λ_{ne} and Λ_{nd} correspond to the neglected elastic and relaxation eigenvalues, respectively. $\mathbf{T}_{lne}$, $\mathbf{T}_{rne}$, $\mathbf{T}_{lnd}$ and $\mathbf{T}_{rnd}$ are their corresponding left and right eigenvectors. Consequently, the state vector is approximated as $\mathbf{x} \approx \mathbf{T}_{rr}\mathbf{x}_r$ and, using Eqs. (9) and (10), the system (8) may be reduced to

$$\begin{aligned} \dot{\mathbf{x}}_r &= \Lambda_r\mathbf{x}_r + \mathbf{T}_{lr}^T\mathbf{p} \\ \mathbf{y} &= \mathbf{C}\mathbf{T}_{rr}\mathbf{x}_r \end{aligned} \tag{11}$$

4.1.2 Real representation of reduced model

The main disadvantage of the reduced state space system (11) is that its matrices are complex. Fortunately, since all overdamped (relaxation) modes were neglected, all elements of the system (11) are composed of complex conjugates, such that

$$\Lambda_r = \text{diag}(\ldots, \lambda_j, \overline{\lambda}_j, \ldots) \; ; \; \mathbf{T}_{lr}^T\mathbf{p} = \text{col}(\ldots, \varphi_j, \overline{\varphi}_j, \ldots) \; ; \; \mathbf{C}\mathbf{T}_{rr} = \begin{bmatrix} \cdots & \phi_j & \overline{\phi}_j & \cdots \end{bmatrix} \tag{12}$$

where λ_j $(j = 1, \ldots, r)$ are the retained elastic eigenvalues and $\overline{\lambda}_j$ their complex conjugates. To construct a real representation of the state space system (11), one may use a state transformation $\hat{\mathbf{x}} = \mathbf{T}_c\mathbf{x}_r$, where $\mathbf{T}_c$ is defined as (Friot and Bouc, 1996)

$$\mathbf{T}_c = \begin{bmatrix} \ddots & & & & \\ & -\mathrm{j}\frac{1}{2\Im(\lambda_j)} & \mathrm{j}\frac{1}{2\Im(\lambda_j)} & & \\ & & & \ddots & \\ \ddots & & & & \\ & \frac{1}{2} - \mathrm{j}\frac{1}{2}\frac{\Re(\lambda_j)}{\Im(\lambda_j)} & \frac{1}{2} + \mathrm{j}\frac{1}{2}\frac{\Re(\lambda_j)}{\Im(\lambda_j)} & & \\ & & & \ddots & \end{bmatrix} \tag{13}$$

so that the real state space system equivalent to Eq. (11) is

$$\begin{aligned} \dot{\hat{\mathbf{x}}} &= \hat{\mathbf{A}}\hat{\mathbf{x}} + \hat{\mathbf{p}} \\ \mathbf{y} &= \hat{\mathbf{C}}\hat{\mathbf{x}} \end{aligned} \tag{14}$$

where

$$\hat{\mathbf{A}} = \mathbf{T}_c\Lambda_r\mathbf{T}_c^{-1} = \begin{bmatrix} & \mathbf{0} & & & \mathbf{I} & \\ \ddots & & & \ddots & & \\ & -|\lambda_j|^2 & & & 2\Re(\lambda_j) & \\ & & \ddots & & & \ddots \end{bmatrix}$$

$$\hat{\mathbf{p}} = \mathbf{T}_c\mathbf{T}_{lr}^T\mathbf{p} \; ; \; \hat{\mathbf{C}} = \mathbf{C}\mathbf{T}_{rr}\mathbf{T}_c^{-1}$$

It is clear that the eigenvalues of the real matrix $\hat{\mathbf{A}}$ are exactly the elements of Λ_r. In the form of Eq. (14), the new state variables $\hat{\mathbf{x}}$ represent the modal displacements and velocities.

4.2 Second order model reduction

The main difficulty in using reduction methods for state space systems, either via modal truncation or balanced realization, is that the dimension of the state space matrix $\mathbf{A}$ may be very large due to the inclusion of internal variables in the FE model. Consequently, when there is a need for repeating the reduced model evaluation for several treatment configurations, which is often the case for control design and optimization, it easily becomes an impractical task. Hence, a novel model reduction method is presented in this section. It consists in reducing the dissipative system (Eq. (6)) before construction of augmented state space system. Since Eq. (6) is already constructed in terms of a modal decomposition of the viscoelastic stiffness matrix $\mathbf{K}_v$, that is, in terms of viscoelastic dissipative modes, one could consider retaining only a few dissipative modes to reduce the augmented system dimension. Obviously, the difficulty would be to guess which dissipative modes to retain.

Let us suppose that the damped solution for the FE dof may be written as $\mathbf{q} = \mathbf{T}_e\hat{\mathbf{q}}$. Replacing this expression in Eq. (6) leads to

$$\mathbf{T}_e^T\mathbf{M}\mathbf{T}_e\ddot{\hat{\mathbf{q}}}+\mathbf{T}_e^T\mathbf{D}\mathbf{T}_e\dot{\hat{\mathbf{q}}}+\mathbf{T}_e^T(\mathbf{K}_e+\mathbf{K}_v^\infty)\mathbf{T}_e\hat{\mathbf{q}}-\mathbf{T}_e^T\mathbf{T}_d\Lambda_d\sum_i\hat{\mathbf{q}}_i^d=\mathbf{T}_e^T\mathbf{F} \tag{15}$$

$$\frac{C_i}{\Omega_i}\Lambda_d\dot{\hat{\mathbf{q}}}_i^d+C_i\Lambda_d\hat{\mathbf{q}}_i^d-\Lambda_d\mathbf{T}_d^T\mathbf{T}_e\hat{\mathbf{q}}=\mathbf{0} \tag{16}$$

Since the null eigenvalues were eliminated from Λ_d, Eq. (16) could also be written as

$$\dot{\hat{\mathbf{q}}}_i^d=-\Omega_i\hat{\mathbf{q}}_i^d+\frac{\Omega_i}{C_i}\mathbf{T}_d^T\mathbf{T}_e\hat{\mathbf{q}} \tag{17}$$

Notice from the last equation that the jk-th element of the matrix $\mathbf{T}_d^T\mathbf{T}_e$ represents the contribution of the k-th response mode to the j-th dissipative mode of the viscoelastic substructure, that is, a measure of how the k-th response mode excites the j-th mode of the viscoelastic substructure. Consequently, supposing that the energy of the overall response is concentrated in certain "response modes", we might be able to identify the viscoelastic modes which are the most excited by the response. Alternatively, from Eq. (15), one may notice that the elements of matrix $\mathbf{T}_e^T\mathbf{T}_d\Lambda_d$ give also a measure of how each viscoelastic dissipative mode contribute to the structural response. Hence, a technique was tested to select some viscoelastic dissipative modes based on their contribution to the dynamics of the overall structure.

Let us define the matrix $\mathbf{R}$ as

$$\mathbf{R}=\Lambda_d\mathbf{T}_d^T\mathbf{T}_e \tag{18}$$

such that its elements R_{jk} represent the weighted residuals between viscoelastic dissipative mode $\mathbf{T}_d^j$ and structural mode $\mathbf{T}_e^k$. Supposing that the majority of structural response energy is contained in the first N_k modes in $\mathbf{T}_e$, the selection of the dissipative modes that contribute the most to the structural response may be performed through the sorting of the following residual vector $\mathbf{r}$

$$r_j=||R_{jk}||,\ \text{for } k=1,...,N_k \tag{19}$$

Notice that each element of $\mathbf{r}$ correspond to a column of $\mathbf{T}_d$, that is a viscoelastic dissipative mode. Thus, it is proposed to eliminate the dissipative modes from $\mathbf{T}_d$ corresponding to the smallest residuals r_j, which are thought to be those that contribute the least to the structural response.

Two main factors determine the performance of the proposed reduction technique: 1) the basis considered for the structural response $\mathbf{T}_e$ and 2) the number of dissipative modes kept in the model. As for the basis considered, let us suppose as a first approximation that the damped modes are similar to the undamped modes. Then, assuming that $\mathbf{T}_e^T\mathbf{M}\mathbf{T}_e=\mathbf{I}$ and $\mathbf{T}_e^T(\mathbf{K}_e+\mathbf{K}_v^\infty)\mathbf{T}_e=\Lambda_e$, Eqs. (15) and (16) can be rewritten as

$$\ddot{\hat{\mathbf{q}}}+\mathbf{T}_e^T\mathbf{D}\mathbf{T}_e\dot{\hat{\mathbf{q}}}+\Lambda_e\hat{\mathbf{q}}-\bar{\mathbf{R}}^T\sum_i\hat{\mathbf{q}}_i^d=\mathbf{T}_e^T\mathbf{F} \tag{20}$$

$$\frac{C_i}{\Omega_i}\bar{\Lambda}_d\dot{\hat{\mathbf{q}}}_i^d+C_i\bar{\Lambda}_d\hat{\mathbf{q}}_i^d-\bar{\mathbf{R}}\hat{\mathbf{q}}=\mathbf{0} \tag{21}$$

Combination of Eqs. (20) and (21) leads then to a reduced-order augmented system

$$\bar{\mathbf{M}}\ddot{\bar{\mathbf{q}}}+\bar{\mathbf{D}}\dot{\bar{\mathbf{q}}}+\bar{\mathbf{K}}\bar{\mathbf{q}}=\bar{\mathbf{F}} \tag{22}$$

with

$$\bar{\mathbf{M}}=\begin{bmatrix}\mathbf{I} & \mathbf{0}\\ \mathbf{0} & \mathbf{0}\end{bmatrix}\ ;\ \bar{\mathbf{D}}=\begin{bmatrix}\mathbf{T}_e^T\mathbf{D}\mathbf{T}_e & \mathbf{0}\\ \mathbf{0} & \mathbf{D}_{dd}\end{bmatrix}\ ;\ \bar{\mathbf{F}}=\begin{Bmatrix}\mathbf{T}_e^T\mathbf{F}\\ \mathbf{0}\end{Bmatrix}$$

$$\bar{\mathbf{K}}=\begin{bmatrix}\Lambda_e & \mathbf{K}_{ed}\\ \mathbf{K}_{ed}^T & \mathbf{K}_{dd}\end{bmatrix}\ ;\ \bar{\mathbf{q}}=\text{col}\left(\hat{\mathbf{q}},\ \hat{\mathbf{q}}_1^d,\ \ldots,\ \hat{\mathbf{q}}_n^d\right)$$

where,

$$\mathbf{D}_{dd}=\text{diag}\left(\frac{C_1}{\Omega_1}\bar{\Lambda}_d\ \cdots\ \frac{C_n}{\Omega_n}\bar{\Lambda}_d\right)\ ;\ \mathbf{K}_{dd}=\text{diag}\left(C_1\bar{\Lambda}_d\ \cdots\ C_n\bar{\Lambda}_d\right)\ ;\ \mathbf{K}_{ed}=\left[-\bar{\mathbf{R}}^T\ \cdots\ -\bar{\mathbf{R}}^T\right]$$

Notice that the structural model is not reduced using its undamped modes $\mathbf{T}_e$, although writing the equations in terms of $\hat{\mathbf{q}}$ instead of $\mathbf{q}$ has some advantages, such as to provide a diagonal structural model, specially if damping matrix $\mathbf{D}$ is a proportional damping such $\mathbf{D}$ will be a diagonal matrix. However, the same technique for reducing the dimension of the dissipative system could still be used with a non-diagonal structural model in Eq. (22). Notice also, from Eq. (22), that the reduced dissipative coordinates $\hat{\mathbf{q}}_i^d$ contain now only those coordinates corresponding to the selected dissipative modes according to their residual and, thus, matrices $\bar{\mathbf{R}}$ and $\bar{\Lambda}$ have a reduced dimension. This reduction can be specially

important since each eliminated dissipative mode leads to a reduction of n dof in Eq. (22), where n is the number of ADF series terms considered (generally at least 3).

The state space system matrices and vectors can then be rewritten as

$$\mathbf{A} = \begin{bmatrix} \mathbf{0} & \mathbf{0} & \cdots & \mathbf{0} & \mathbf{I} \\ \frac{\Omega_1}{C_1}\bar{\mathbf{T}}_d^T\mathbf{T}_e & -\Omega_1\mathbf{I} & & \mathbf{0} & \mathbf{0} \\ \vdots & & \ddots & & \mathbf{0} \\ \frac{\Omega_n}{C_n}\bar{\mathbf{T}}_d^T\mathbf{T}_e & \mathbf{0} & & -\Omega_n\mathbf{I} & \mathbf{0} \\ -\Lambda_e & \bar{\mathbf{R}}^T & \cdots & \bar{\mathbf{R}}^T & -\mathbf{T}_e^T\mathbf{D}\mathbf{T}_e \end{bmatrix}$$

$$\mathbf{x} = \begin{bmatrix} \bar{\mathbf{q}} \\ \dot{\bar{\mathbf{q}}} \end{bmatrix} \; ; \; \mathbf{p} = \begin{bmatrix} \mathbf{0} \\ \mathbf{T}_e^T\mathbf{F} \end{bmatrix} \; ; \; \mathbf{C} = [\mathbf{C}_{\bar{q}}\mathbf{T}_e \quad \mathbf{C}_{\dot{q}}\mathbf{T}_e]$$

These, now reduced, state space system matrices can then be further reduced through the state space model reduction presented previously, possibly saving a large amount of computation time. In the next section, the technique presented here is validated for a cantilever beam with viscoelastic treatment. Also an analysis of the number of dissipative modes that should be kept in the model is presented.

5 Validation of reduced order models

Let us consider the aluminum cantilever beam partially covered with a constrained layer treatment as presented in Fig. 1. The beam is of length 300 mm and thickness 1 mm and is made of aluminum with Young's modulus 70 GPa and mass density 2700 kg/m^3. No viscous damping is considered in this example, that is $\mathbf{D} = \mathbf{0}$. The constraining layer is also made of aluminum and has thickness 0.5 mm and length 270 mm, that is the treatment covers 90% of the beam. The viscoelastic layer has thickness 0.254 mm (10 mil) and is made of 3M ISD112 viscoelastic material, with a mass density of 1000 kg/m^3. The viscoelastic material shear modulus is frequency-dependent. The curve-fitting of ADF parameters to the measured shear modulus provided by 3M is presented in the next section.

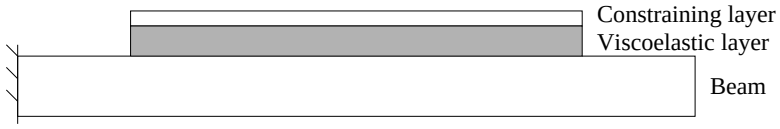

Figure 1: Cantilever beam partially covered with a passive constrained layer damping treatment.

The FE model is obtained using 35 sandwich beam elements, with 6 dof per node, leading to a total of 105 mechanical dof (for details on the FE model, please refer to Trindade, Benjeddou and Ohayon, 2001a). The FE mesh is presented in Fig. 2. The beam is also subjected to an impact mechanical force at 10 mm from the clamped end and its response is measured at the same point.

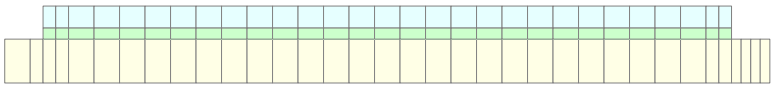

Figure 2: Finite element mesh considered for the cantilever beam with constrained viscoelastic treatment.

5.1 Curve fitting of viscoelastic material properties

The ADF parameters G_0, Δ_i and Ω_i must be curve-fitted relative to the measurements of $G^*(\omega)$. In the present work, a nonlinear least squares optimization method was used to evaluate the ADF parameters. Figure 3 shows the measured and approximated storage modulus (G') and loss factor (η) for 3M ISD112 viscoelastic material at 20^{o}C, where

$$G^*(\omega) = G'(\omega) + \mathrm{j}G''(\omega) = G'(\omega)[1 + \mathrm{j}\eta(\omega)] \tag{23}$$

As shown in Fig. 3, both storage modulus and loss factor are well represented by five series terms of ADF parameters, whereas three ADF series terms provide only a first approximation (within 15% error margin) for the frequency-dependence. Nevertheless, these parameters are valid only in the frequency-range considered, that is the frequency-range for which material properties were furnished by 3M. Therefore, it is necessary to ensure a reasonable behavior of estimated material properties outside the frequency-range, since arbitrary external perturbations will generally excite modes lying on this interval. Required asymptotical properties are

$$\begin{cases} \lim\limits_{\omega\to 0} G^*(\omega) = G_0 \\ \lim\limits_{\omega\to\infty} G^*(\omega) = G_\infty \end{cases}, \quad \text{where } G_\infty > G_0 \in \mathbb{R}^+ \tag{24}$$

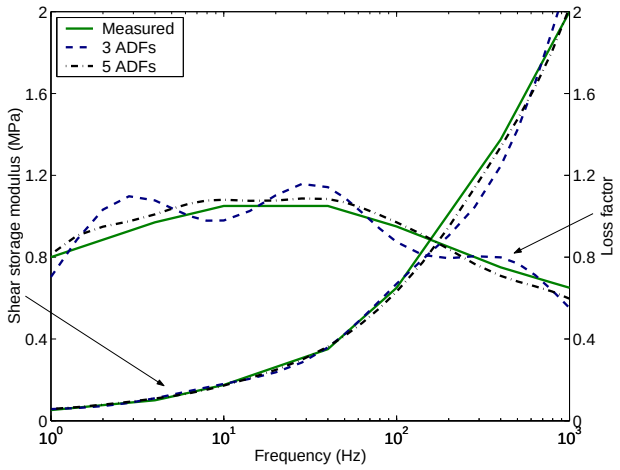

Figure 3: Frequency-dependence of 3M ISD112 viscoelastic material properties at 20°C (solid line) and curve-fit using three ADF series terms (dashed line) and five ADF series terms (dashed-dotted line).

Table 1: Curve-fitted ADF parameters for viscoelastic material 3M ISD112 at 20°C.

	ADF with 3 series terms			ADF with 5 series terms		
i	G_0 (MPa)	Δ_i	Ω_i (rad/s)	G_0 (MPa)	Δ_i	Ω_i (rad/s)
1	0.0511	2.8164	31.1176	0.0440	1.3545	12.4547
2		13.1162	446.4542		3.2610	73.8749
3		45.4655	5502.5318		7.7741	387.4302
4		–	–		18.9495	1472.7588
5		–	–		49.7732	9791.3957

Meaning that the shear modulus tends to its static (relaxed) and instantaneous (unrelaxed) values at the boundaries 0 and ∞, respectively. This also imposes that $\eta(0), \eta(\infty) = 0$, that is, dissipation only occurs in the transition region.

Notice also that these properties are valid for a temperature of 20°C and it is well-known that temperature decrease will move these master curves to the left and vice-versa. On the other hand, some viscoelastic materials present optimal loss factor at lower frequencies. So that it is normally possible to select a material according to frequency-range of interest and operation temperature.

5.2 Comparison of reduced and full order dissipative models

The reduced state space systems, with and without previous reduction of the dissipative system, are now compared for the cantilever beam introduced previously. Five series terms of ADF parameters were considered in both cases, leading to an inclusion of 445 dissipative dof (89 dof $\times$ 5 ADF series terms) in addition to the 105 mechanical dof from the FE model.

Figures 4 and 5 present the average eigenfrequency and modal damping factor errors, respectively, when using different numbers of dissipative modes, corresponding to the largest residuals, compared to using all but rigid body dissipative modes. Notice that for the sake of clarity in comparison, the first ten vibration modes were grouped, such that the error shown for *Modes 1-3* in Fig. 4, for instance, corresponds to the average of the eigenfrequency errors for eigenmodes 1, 2 and 3. Comparison of Figs. 4 and 5 shows that the eigenfrequency errors are much smaller than that for the damping factors. This is probably due to the fact that the dissipative coordinates are solely responsible for the damping in the structure and neglecting all dissipative modes leads to the absence of damping. Moreover, although the damping factor error decreases quite rapidly for modes 4-10, it is still larger than 40% for modes 1-3 when using less than 19 dissipative modes. Nevertheless, when using 30 dissipative modes the damping errors decrease to 0.0778% (Modes 1-3), 0.1210% (Modes 4-6) and 0.2259% (Modes 7-10), while the eigenfrequency errors are as low as 0.0033% (Modes 1-3), 0.0101% (Modes 4-6) and 0.0081% (Modes 7-10). Indeed, from Fig. 6, one can observe that the 31^{th} largest residual is only 0.6% of the first one so that most of the coupling between elastic and dissipative coordinates are provided by the first 30 dissipative modes. Alternatively, one may observe, from Fig. 7, that the cumulative sum of the normalized residuals is more than 99% for 30 dissipative modes.

Figure 8 shows the frequency response function between the impact force input and displacement output, both colocated at 10 mm from the clamped end, using all but rigid body dissipative modes, as a reference, and reduced-order models using only 9, 19 and 29 dissipative modes of the 89 available. It is possible to observe that higher-frequency modes are better represented by low-order models as previously showed in frequency and damping errors analyses. It can be seen that, when using only 9 dissipative modes, the frequency response around the first, second and fourth eigenfrequencies is not correctly represented. However, when including 19 dissipative modes, the difference between the reduced-order model and the full-dissipative model is almost only perceptible around the first eigenfrequency. The frequency response for the reduced-order model with 29 dissipative modes matches almost exactly the full-dissipative model.

As it is guessed that the importance of the dissipative coordinates in the representation of damping may be depen-

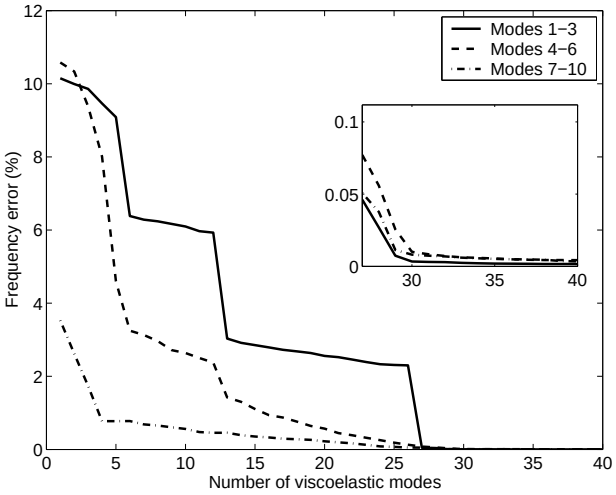

Figure 4: Average eigenfrequency error when using different numbers of dissipative modes in second order system compared to using all but rigid body modes.

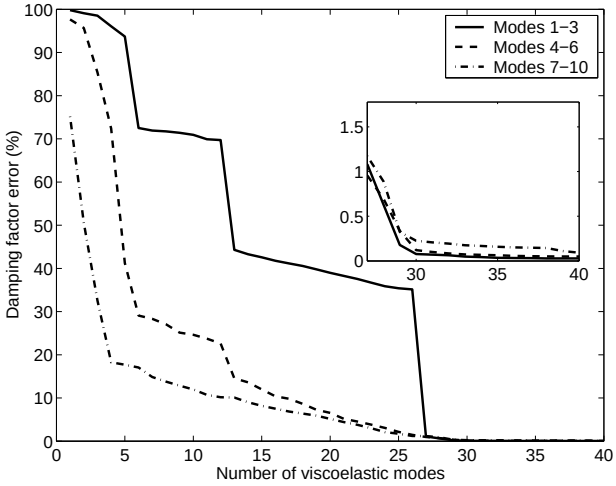

Figure 5: Average damping factor error when using different numbers of dissipative modes in second order system compared to using all but rigid body modes.

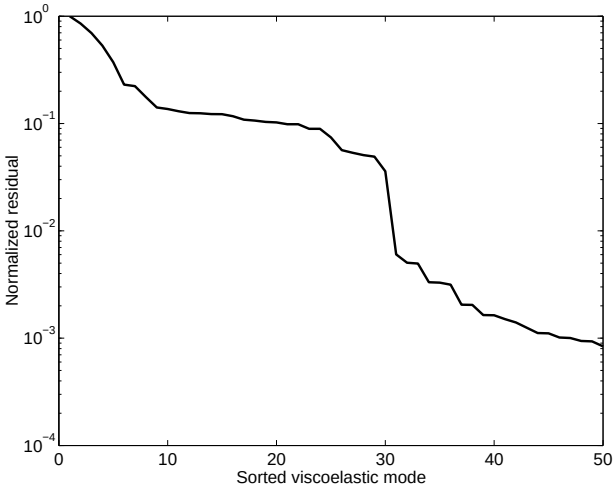

Figure 6: Normalized residual for each viscoelastic dissipative mode.

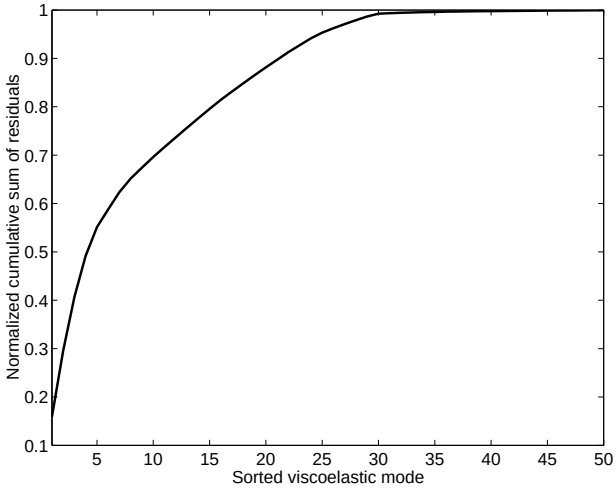

Figure 7: Cumulative sum of residuals for the dissipative modes.

dent on the overall damping level induced in the structure by the viscoelastic damping treatment, a similar analysis was performed for a cantilever beam with only 50% of area covered with the viscoelastic treatment. This is done by changing the length of the viscoelastic and constraining layers to 150 mm in Fig. 1, whereas still centered in the beam surface. This leads to a much less damped structure, such that the 10 first modal damping factors are $\zeta(50\%) = [5.6, 9.2, 5.3, 5.2, 6.7, 5.3, 4.7, 4.7, 3.8, 2.8]\%$ compared to $\zeta(90\%) = [5.8, 11.2, 11.7, 11.8, 11.6, 10.8, 9.4, 7.8, 6.3, 5.1]\%$ of the previous configuration.

Similarly to the previous case, Figs. 9 and 10 present the average eigenfrequency and modal damping factor errors, respectively, when using different numbers of dissipative modes, corresponding to the largest residuals, compared to using all but rigid body dissipative modes. For this case, the eigenfrequency errors are also much smaller than that for the damping factors. Here, both the eigenfrequency and damping factor errors decrease more rapidly than in the previous case. It may be guessed that this is due to the fact that a less damped structure requires less dissipative coordinates. Indeed, in this case, only 18 dissipative modes are required to reduce the damping error to less than 1% for all ten first vibration modes. Indeed, when using 18 dissipative modes, the damping errors are 0.7589% (Modes 1-3), 0.1456% (Modes 4-6) and 0.2066% (Modes 7-10) and the eigenfrequency errors are 0.0458% (Modes 1-3), 0.0087% (Modes 4-6) and 0.0044% (Modes 7-10). Also, as in the previous case, the cumulative sum of the normalized residuals is more than 99%.

For the case of 50% coverture, the frequency response function was also analyzed, and shown in Fig. 11, using all but rigid body dissipative modes, as a reference, and reduced-order models using only 5, 9 and 18 dissipative modes of the 52 available. For this case, the higher-frequency modes are also better represented by low-order models and when using a reduced-order model with 18 dissipative modes the frequency response function matches almost exactly the full-dissipative model.

Although, for a less damped structure, less dissipative modes were necessary to represent correctly its viscoelastic damping, it is worthwhile noticing that, for the structure with smaller coverture, there are less dissipative coordinates to

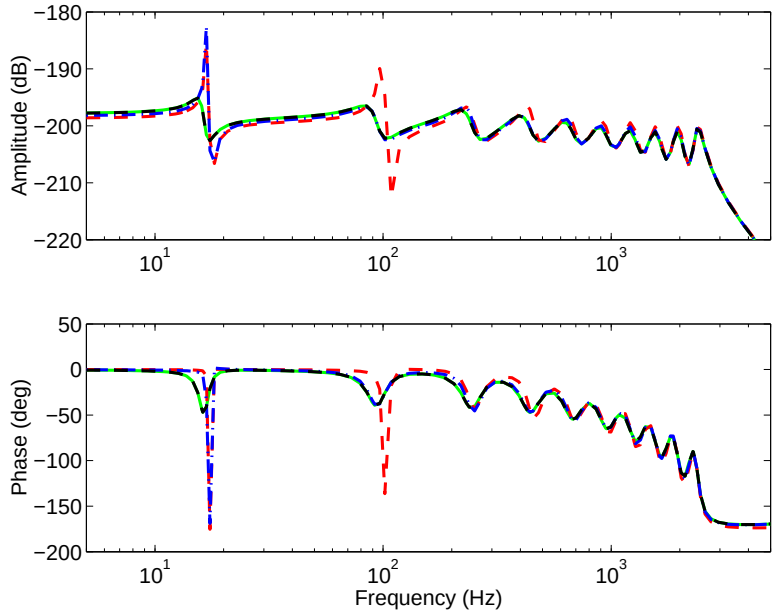

Figure 8: Frequency response function using different numbers of dissipative modes in second order system. –: all but rigid body modes (89), - -: 9 modes, -.: 19 modes, – –: 29 modes.

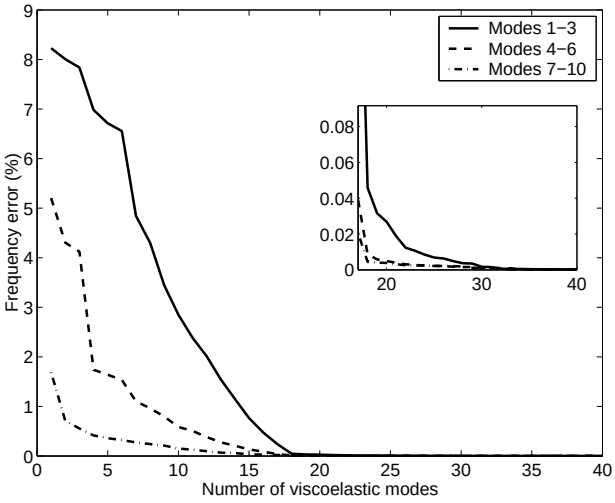

Figure 9: Average eigenfrequency error when using different numbers of dissipative modes in second order system compared to using all but rigid body modes.

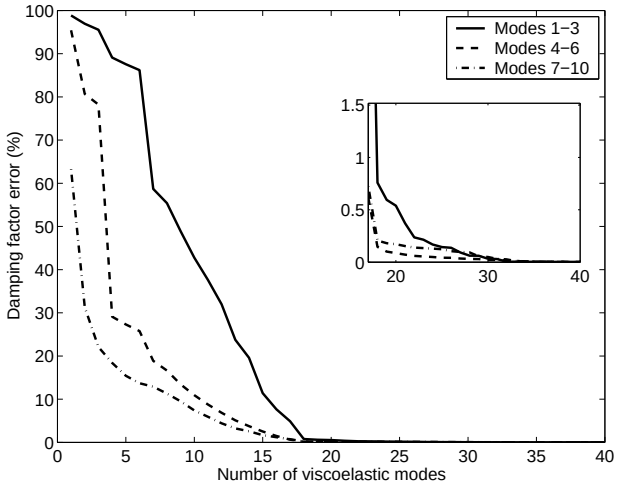

Figure 10: Average damping factor error when using different numbers of dissipative modes in second order system compared to using all but rigid body modes.

be reduced. This is due to the fact that there are more rigid body dissipative modes, corresponding to the mechanical dof of the beam uncovered areas. Notice however that in both cases it is possible to reduce the number of viscoelastic modes to approximately one third of all non-rigid body ones. Since 5 ADF series terms were necessary to correctly represent the frequency-dependence of the viscoelastic material, that reduction represents a gain of 300 dof (reduction from 655 dof to 355 dof) in the state space system for the 90% coverture case. Since the calculation of the eigenvalues of the state space matrix requires a number of operations approximately equal to N^3, where N is the matrix size, this reduction would lead to a reduction in 84% of computational effort.

6 Conclusions

The present work has presented an alternative reduction method for internal variables-based viscoelastic finite element models. A previously developed sandwich/multilayer beam finite element model combined to the internal variables-based Anelastic Displacement Fields viscoelastic model was used. Through a physical interpretation of the dissipative modes, due to the added internal variables, and their coupling with structural vibration modes in the second-order model, a technique for the reduction of the extra dissipative coordinates before transformation to the state space system was proposed. This method has led to much faster computations on the reduction of the state space system at the second reduction phase. Comparison between the reduced-order model and full-dissipative models for a clamped beam with passive constrained layer damping treatment has shown satisfactory results. In particular, a reduction of 67% of dissipative

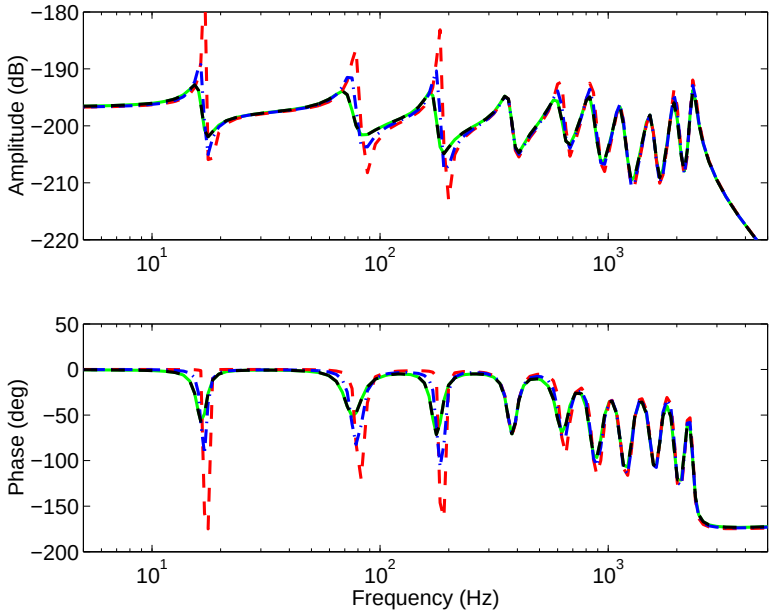

Figure 11: Frequency response function using different numbers of dissipative modes in second order system. –: all but rigid body modes (52), - -: 5 modes, -.: 9 modes, – –: 18 modes.

dof has led to errors smaller than 0.5% for damping factors of the coupled structure.

7 References

Friot, E. and Bouc, R., 1996, "Contrôle optimal par rétroaction du rayonnement d'une plaque munie de capteurs et d'actionneurs piézo-électriques non colocalisés", 2^{eme} Colloque GDR Vibroacoustique, LMA, Marseille, pp. 229–248.

Friswell, M.I. and Inman, D.J., 1999, "Reduced-order models of structures with viscoelastic components", AIAA Journal, Vol.37, No.10, pp.1318–1325.

Golla, D.F. and Hughes, P.C., 1985, "Dynamics of viscoelastic structures – a time-domain, finite element formulation", Journal of Applied Mechanics, Vol.52, No.4, pp.897–906.

Lesieutre, G.A. and Bianchini, E., 1995, "Time domain modeling of linear viscoelasticity using anelastic displacement fields", Journal of Vibration and Acoustics, Vol.117, No.4, pp.424–430.

McTavish, D.J. and Hughes, P.C., 1993, "Modeling of linear viscoelastic space structures", Journal of Vibration and Acoustics, Vol.115, pp.103–110.

Park, C.H., Inman, D.J. and Lam, M.J., 1999, "Model reduction of viscoelastic finite element models", Journal of Sound and Vibration, Vol.219, No.4, pp.619–637.

Trindade, M.A. and Benjeddou, A., 2002, "Hybrid active-passive damping treatments using viscoelastic and piezoelectric materials: review and assessment", Journal of Vibration and Control, Vol.8, No.6, pp.699–746.

Trindade, M.A., Benjeddou, A. and Ohayon, R., 2000, "Modeling of frequency-dependent viscoelastic materials for active-passive vibration damping", Journal of Vibration and Acoustics, Vol.122, No.2, pp.169–174.

Trindade, M.A., Benjeddou, A. and Ohayon, R., 2001a, "Finite element modeling of hybrid active-passive vibration damping of multilayer piezoelectric sandwich beams. part 1: Formulation and part 2: System analysis", International Journal for Numerical Methods in Engineering, Vol.51, No.7, pp.835–864.

Trindade, M.A., Benjeddou, A. and Ohayon, R., 2001b, "Piezoelectric active vibration control of sandwich damped beams", Journal of Sound and Vibration, Vol.246, No.4, pp.653–677.

8 Responsibility notice

The author is the only responsible for the printed material included in this paper.